Significance of incongruent DNA loci in the taxonomy of wood-decaying Basidioradulum radula

Viner, Ilya

2021-09-03

Viner , I , Kokaeva , L , Spirin , V & Miettinen , O 2021 , ' Significance of incongruent DNA loci in the taxonomy of wood-decaying Basidioradulum radula ' , Mycologia , vol. 113 , no. 5 , pp. 995-1008 . https://doi.org/10.1080/00275514.2021.1930449

http://hdl.handle.net/10138/341557
https://doi.org/10.1080/00275514.2021.1930449

MYCOLOGIA

Mycologia

ISSN: (Print) (Online) Journal homepage: https://www.tandfonline.com/loi/umyc20

Significance of incongruent DNA loci in the taxonomy of wood-decaying *Basidioradulum radula*

Ilya Viner, Lyudmila Kokaeva, Viacheslav Spirin & Otto Miettinen

To cite this article: Ilya Viner, Lyudmila Kokaeva, Viacheslav Spirin & Otto Miettinen (2021) Significance of incongruent DNA loci in the taxonomy of wood-decaying *Basidioradulum radula*, Mycologia, 113:5, 995-1008, DOI: 10.1080/00275514.2021.1930449

To link to this article: https://doi.org/10.1080/00275514.2021.1930449

MYCOLOGIA
2021, VOL. 113, NO. 5, 995–1008
https://doi.org/10.1080/00275514.2021.1930449

Taylor & Francis
Taylor & Francis Group

Significance of incongruent DNA loci in the taxonomy of wood-decaying *Basidioradulum radula*

Ilya Viner [a,b], Lyudmila Kokaeva [b], Viacheslav Spirin [a], and Otto Miettinen [a]

[a]Botanical Museum, Finnish Museum of Natural History, University of Helsinki, P.O. Box 7, 00014, Finland; [b]Faculty of Biology, Lomonosov State University, Leninskie Gory 1/12, 119234 Moscow, Russia

ABSTRACT

Modern taxonomic studies of Agaricomycetes rely on the integrative analyses of morphology, environmental data, geographic distribution, and usually several DNA loci. However, sampling and selection of DNA loci for the analyses are commonly shallow. In this study, we suggest minimal numbers of necessary specimens to sample and DNA loci to analyze in order to prevent inadequate taxonomic decisions in species groups with minor morphological and genealogical differences. We sampled four unlinked nuclear DNA gene regions (nuc rDNA ITS1-5.8S-ITS2, *gh63, rpb2*, and *tef1*) to revise the systematics of a common wood-decaying species *Basidioradulum radula* (Hymenochaetales) on an intercontinental set of specimens collected in the Northern Hemisphere. The DNA loci analyzed violate the genealogical concordance phylogenetic species recognition principles, thus confirming a single-species interpretation. We conclude that *Hyphodontia syringae* is a younger synonym of *B. radula*.

ARTICLE HISTORY
Received 27 September 2020
Accepted 12 May 2021

KEYWORDS
Basidiomycota; *Hyphodontia syringae*; morphological plasticity; phylogenetic incongruence; phylogeography; taxonomy

INTRODUCTION

Historically, the taxonomic treatment of Agaricomycetes was mainly based on the morphology of basidiomata. Later, the adoption of molecular techniques and particularly the widespread use of nuc rDNA internal transcribed spacer region ITS1-5.8S-ITS2 (ITS) have shown that morphological traits do not necessarily provide meaningful phylogenetic and systematic signals. Further advances in fungal genetics have established the idea that systematic studies may suffer from ignoring differing genealogies of unlinked loci (Taylor et al. 2000; Giraud et al. 2008). This may result in topologically different individual gene trees. In such situations, a single strictly bifurcating tree (consensus or concatenated multilocus) is not able to show the convoluted genealogies of such phylogenetically incompatible loci. Following Leigh et al. (2008), we will refer to these as incongruent loci.

But is accounting for unlinked loci relevant for practical taxonomy? At present, many systematic studies of Agaricomycetes rely on a limited number of unlinked DNA loci. Since 2015, among 162 systematic papers featuring Hymenochaetales—a medium-sized order of Agaricomycetes—only 23% have used more than one unlinked DNA locus. Even in 2020s this percentage has remained low—30% (as of 1 May 2021). Species delimitations based on one DNA marker may still be reliable if propped up by integrative analyses of morphology, environmental data, geographic distribution, and, when available, mating tests. However, ignoring unlinked loci becomes troubling when high morphological variation and incongruence between individual loci coincides, obscuring potential interspecific differences.

Incongruent loci may have dissimilar evolutionary histories due to different phenomena such as incomplete lineage sorting or introgression. Distinguishing these causes has important implications for taxonomic conclusions. Under incomplete lineage sorting, which often occurs in true genetically isolated species, different variants of one DNA locus, haplotypes as we call them here, were already present in the ancestral population. For some stochastic reasons, these haplotypes have not filtered out (or become fixed) in the progeny populations. On the flip side, loci shared via introgression may indicate gene flow between populations within a single species with a strong population structure. Although not being a decisive argument, clear signs of gene flow between diverged populations may tip the scales in favor of a one species interpretation.

Although the divergence time of haplotypes under lineage sorting is older than the emergence of the progeny populations, this does not hold for haplotypes that have become fixed and only later have been shared via introgression. Therefore, the genetic distance between haplotypes (and branch lengths of gene trees) under introgression is expected to be smaller than under incomplete lineage sorting (Holder et al. 2001).

CONTACT Ilya Viner ilya.viner@helsinki.fi

Published online 08 Jul 2021

If lineage sorting is adequately addressed, comparison of phylogenies of more than one locus for species recognition can be applied. When incongruence between loci is caused by recombination among individuals, the transition from conflict to topological uniformity between individual gene trees can be interpreted as a species boundary. Taylor et al. (2000) called this concept genealogical concordance phylogenetic species recognition. Here, we implement this approach on *Basidioradulum radula* (Fr.) Nobles, a morphologically variable corticioid species widely distributed in the holarctic.

The initial incentive for this study emerged from analysis of fresh collections of *Hyphodontia syringae* Langer, a polypore species described from China. Our preliminary morphological observations and phylogenetic analysis of nuc 28S rDNA (28S) showed that *H. syringae* belonged to the genus *Basidioradulum* Nobles. Moreover, the 28S of these two species were almost identical, which suggested at most a recent divergence of these two species. Prior mating experiments on *B. radula* have suggested a species with an intercontinental distribution (Nobles 1967), but we had no access to mating data for *H. syringae*. In order to clarify the systematic status of *H. syringae*, we conducted phylogenetic analyses based on four unlinked genetic loci (*gh63*, ITS, *rpb2*, and *tef1*) on a comprehensive set of *B. radula* and *H. syringae* specimens collected from diverse woody substrates in North America and Eurasia.

MATERIALS AND METHODS

Morphological methods.—Type material and specimens from the herbarium of the University of Helsinki (H) were studied. Microscopic methods were described in Miettinen et al. (2006). All measurements were made in Cotton blue (CB; Merck 1275; Kenilworth, New Jersey) with phase contrast illumination (1250×). The following abbreviations were used in microscopic descriptions: L = mean spore length; W = mean spore width; Q = mean L/W ratio; n = number of basidiospores (basidia, cystidia, hyphae) measured per number of specimens. We excluded 5% of measurements from each end of the range representing variation of basidiospores and cystidia. Excluded extreme values were indicated in parentheses when they differed from the lower or higher 95% percentile.

DNA extraction and sequencing.—Total genomic DNA was extracted from herbarium specimens using the E.Z.N.A. Forensic DNA Kit (Omega Bio-tek, Norcross, Georgia) according to the manufacturer's instructions or standard cetyltrimethylammonium bromide (CTAB)–chloroform extraction. Primers used to amplify the complete ITS region were ITS1F+ITS4 (White et al. 1990; Gardes and Bruns 1993), and for the nuc 28S rDNA (28S) region we used LR0R+LR5 (Vilgalys and Hester 1990; Rehner and Samuels 1994). Primers used for a portion of glycoside hydrolase (*gh63*) were *gh63*IF+*gh63*IR (Pérez-Izquierdo et al. 2017); for a portion of the translation elongation factor 1-alpha (*tef1*), primers 983F+2218R (Rehner and Buckley 2005) were used; and for the most variable region of the second largest subunit of RNA polymerase II (*rpb2*), primers bRPB2-6f+bRPB2-7.1R (Matheny 2005) were used. After amplification, polymerase chain reaction (PCR) products were run on a 1.5% agarose gel stained with ethidium bromide or GelRed staining (Biotium, Fremont, California) and visualized under ultraviolet (UV) light. PCR products were purified from agarose gels using a Fermentas Genomic DNA Purification Kit (Thermo Fisher Scientific, Waltham, Massachusetts). Sequencing reactions were performed on an ABI model 3130 genetic analyzer (Applied Biosystems, Foster City, California) and BigDye 3.1 and on an ABI 3730xl analyzer (Applied Biosystems) by Macrogen (Amsterdam, the Netherlands).

Deciphering of chromatograms.—Insertion/deletion events in a diploid genome result in one of the DNA templates containing extra nucleotide positions. The corresponding Sanger sequencing chromatogram was translated as double peaks with heterozygous bases because the two DNA templates were superimposed with a shift of the fixed length of the insertion/deletion after the mutation site. Such pieces of chromatograms cannot be read directly and often are discarded. There is, however, simple logic to decode them into two different length haplotypes. This process has been described and implemented in several software packages (Dmitriev and Rakitov 2008; Zhidkov et al. 2011; Chang et al. 2012).

We performed this procedure manually, since there were only a few such chromatograms produced for this study. The reverse-complement chromatograms were utilized as well in order to double-check the accuracy of the decoded haplotypes and to verify whether there was only one indel in a chromatogram or more. In case of only one indel, both forward and reverse reads yielded clean chromatograms up to the indel from both sides. This method allowed us to detect a number of *Basidioradulum radula* samples producing at least two haplotypes in ITS and *tef1* sequences. We discarded two ITS sequences because they had more than one indel. As a result, we deciphered and included in the analyses two ITS haplotypes from four samples, distinguished by

different 1–2-bp indels in ITS1 or ITS2, and two *tef1* haplotypes from three samples marked by a 5-bp indel in an intron.

This deciphering approach cannot be applied if two templates have the same length; thus, substitution mutations are indicated as double peaks scattered on a clean chromatogram. In this case, accurately assigning each peak from the pair to one of the initial templates is impossible based on this chromatogram only. One of the *B. radula* samples, Himelbrant 2013, yielded such an *rpb2* chromatogram. It lacked an insertion/deletion mutation but showed heterozygous bases at many nucleotide positions, unlike the other nonpolymorphic *rpb2* sequences. In order not to introduce two hypothetical haplotypes for Himelbrant 2013, we discarded this sequence from further phylogenetic analyses. With that and inclusion of both deciphered haplotypes for samples bearing insertion/deletion mutations, we ended up with different numbers of sequences across the four loci: 15 ITS, 18 *gh63*, 17 *tef1*, and 14 *rpb2* sequences. Two 28S were also produced for a preliminary analysis, which is not given here. All newly produced sequences have been deposited in GenBank (TABLE 1).

Phylogenetic analyses.—We constructed four data sets (*gh63*, ITS, *rpb2, tef1*) including exons and introns. Alignments were calculated through the MAFFT 7.429 online server (https://mafft.cbrc.jp/alignment/server/) using the L-INS-i strategy (Katoh et al. 2017). After removing unaligned 5′ and 3′ tails, the final alignments (TABLE 2) were deposited at TreeBASE (TB2:S25768).

We performed hierarchical likelihood ratio tests for phylogenetic congruence with Concaterpillar 1.7.2 (Leigh et al. 2008) in order to test whether the studied loci were congruent and thus able to be concatenated. For this, an alpha level of 0.05 together with the GTR substitution model was used.

We inferred midpoint-rooted phylogenetic trees with maximum likelihood (ML) and Bayesian inference (BI). Nucleotide substitution models were chosen with TOPALI 2.5 (Milne et al. 2008) based on the Bayesian information criterion (BIC). We performed BI using MrBayes 3.2 (Ronquist et al. 2012). In these analyses, three parallel runs with four chains each and other default parameters were run for 1 million generations. A burn-in of 25% was used in the final analyses, ensuring that the average standard deviation of split frequencies had reached <0.01 for all data sets. Support at nodes was indicated when posterior probabilities were ≥0.9. ML analysis was performed in RAxML 7.2.8 (Stamatakis 2006) implemented in Geneious 9.1.8 (http://www.geneious.com) (Kearse et al. 2012). Among available evolutionary models, we preferred to use the GTR model with a gamma correction (GTRGAMMA) according to the RAxML user manual. Bootstrapping was performed using the rapid bootstrapping algorithm, with the number of bootstrap replicates set to 1000. Support at nodes was indicated with bootstrap values ≥80%.

We compared phylogenetic trees of the three protein coding loci (*gh63, rpb2, tef1*) using tanglegrams. Tanglegrams show the trees depicted with the tips facing each other so that corresponding samples are connected by lines. The degree to which lines cross gives an approximate but vivid grasp of topological tree difference.

RESULTS

Patterns of polymorphism in sequence data.—Each set of protein-coding loci (*gh63, rpb2, tef1*) consisted of two well-discernible groups, or haplotype groups, distinguished by five to nine sites that happened to be phylogenetically informative (TABLE 2). These haplotype groups did not correspond between the loci (FIG. 1). Furthermore, samples with polymorphic *tef1* contained both of the *tef1* haplotype groups. There were no such clear haplotype groups for *B. radula* and *H. syringae* in ITS. Only south Chinese samples could be discerned as such, although they were distinguished only by one substitution mutation and a 2-bp indel in ITS2.

As expected at this taxonomic scale, the studied loci were polymorphic mostly in the noncoding regions and at third-codon positions. However, there were a few nonsynonymous substitution mutations (TABLE 2). Three of them were highly important for the analyses, as they distinguished the two haplotype groups of *gh63*.

Gene trees.—All studied loci were found to be incongruent with each other. Therefore, we analyzed the four genetic loci (*gh63*, ITS, *rpb2, tef1*) separately and avoided gene concatenation. The best evolutionary model for all the analyzed data sets was K80. We present here only the BI topology, since it was nearly the same as ML topology.

In all cases, the analyses resolved two well-supported clades (FIGS. 2, 3, 4, and 5), but the resulting trees were topologically different, as they shared no clades at the deepest split. For *gh63, rpb2*, and *tef1*, these clades coincided with the abovementioned haplotype groups (FIG. 1; TABLE 2). Even the apparent similarity between *gh63* and *rpb2* phylogenies was undermined by two samples, Spirin 3770 and Himelbrant 2016, which ended up in noncorresponding clades (FIG. 3). Furthermore, the *tef1* tree was noticeably incongruent with all other gene trees (FIGS. 4 and 5).

Table 1. Specimens, GenBank, and UNITE accession numbers (marked by asterisk) for DNA sequences used in this study (new sequences are in bold).

		Accession numbers				
Specimen	Species	ITS	*gh63*	*rpb2*	*tef1*	28S
asp 2	*B. radula*	AY382822				
CBS 112.40	*B. radula*	MH856054				
Dai 1215B Holotype	*H. syringae*		**MT333842**			
DLL 2011-281	*B. radula*	KJ140758				
GEL 2493	*B. radula*	DQ234537				
Härkönen K320	*B. radula*	**MT341253**	**MT333841**	**MT333813**	**MT333790**	**MT355800**
Himelbrant 2016	*B. radula*	**MT341260**	**MT333832**	**MT333814**	**MT333800**	
Himelbrant 2013	*B. radula*		**MT333833**	**MT333817**	**MT333798**	
					MT333799	
Kotiranta 26121	*B. radula*	**MT341261**	**MT333831**	**MT333815**	**MT333801**	
KUC 20121019_21	*B. radula*	KJ668571				
KUN 1510	*B. radula*		**MT333837**	**MT333821**	**MT333794**	
Kunttu 8629	*B. radula*	**MT341254**	**MT333839**	**MT333810**	**MT333792**	
LWZ 20180510-18	*B. mayi*	MN017785				
LWZ 20180510-23	*B. mayi*	MN017784				
MEL 2385925	*B. tasmanicum*	MN017783				
MEL 2403476	*B. tasmanicum*	MN017781				
MEL 2386000	*B. tasmanicum*	MN017782				
Miettinen 16045	*B. radula*	**MT341265**	**MT333828**		**MT333805**	
		MT341266				
Miettinen 16070	*B. radula*	**MT341264**	**MT333827**	**MT333824**	**MT333806**	
					MT333807	
Miettinen 16071	*B. radula*	**MT341267**	**MT333826**	**MT333818**	**MT333808**	
Miettinen 16076	*B. radula*	**MT341268**	**MT333825**	**MT333819**	**MT333809**	
		MT341269				
OF 253552	*B. radula*	UDB038194*				
OF 253579	*B. radula*	UDB038207*				
OF 260088	*B. radula*	UDB036143*				
Poso 2011	*B. radula*	**MT341255**				
		MT341256				
RM 73	*B. radula*	MK796532				
S 47	*B. radula*	FJ820535				
Spirin 3770	*B. radula*	**MT341257**	**MT333836**	**MT333812**	**MT333796**	
Spirin 5631	*H. syringae*	**MT341258**	**MT333835**	**MT333811**	**MT333795**	**MT328752**
		MT341259				
Spirin 8048	*H. syringae*		**MT333834**	**MT333822**	**MT333797**	
Spirin 8489	*B. radula*	**MT358395**	**MT333830**	**MT333820**	**MT333802**	
					MT333803	
Spirin 8500a	*B. radula*	**MT341262**	**MT333829**	**MT333823**	**MT333804**	
		MT341263				
Tortić 7_77	*B. radula*		**MT333840**		**MT333791**	
TU 111280	*B. radula*	UDB034053*				
TU 114705	*B. radula*	UDB0183649*				
TU 117140	*B. radula*	UDB024119*				
TU 117260	*B. radula*	UDB032080*				
TU 117280	*B. radula*	UDB032082*				
UC 2023076	*B. radula*	KP814413				
Uimonen 2013	*B. radula*		**MT333838**	**MT333816**	**MT333793**	
Zhao 1033	*B. radula*	MG231902				
Zhao 1043	*B. radula*	MG231822				
Zhao 5230	*B. radula*	MK268851				
Zhao 5248	*B. radula*	MK404500				
Zhao 974	*B. radula*	MH114924				
Zhao SWFU 006351	*B. radula*	MK809420				

Note. New sequences are in bold.

Table 2. Summary of the four DNA sequence alignments.

Parameter	*gh63*	ITS	*rpb2*	*tef1*
Number of sequences	18	45	14	20
Length of final alignment	429	512	716	892
Number of parsimony informative characters in noncoding regions	2	36	1	14 (8)
Number of parsimony informative characters at the third-codon positions	7 (2)		17 (5)	14 (1)
Number of parsimony informative characters at the first- and second-codon positions	7 (3)			1

Note. Numbers in parentheses indicate parsimony-informative characters distinguishing two main haplotype groups for protein coding loci *gh63, rpb2*, and *tef1*.

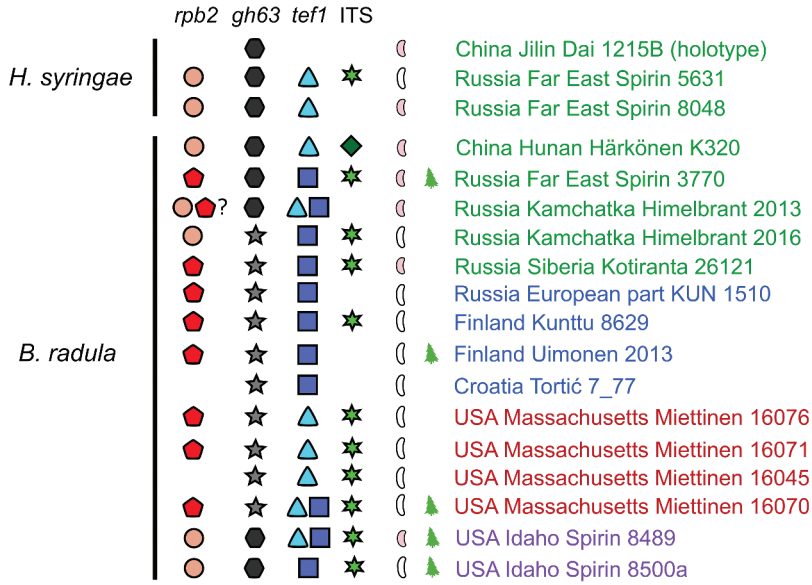

Figure 1. Distribution of haplotype groups across studied DNA loci of *Basidioradulum radulum* and *Hyphodontia syringae*. Different geometric shapes designate haplotype groups; two geometric shapes together indicate both haplotypes present in the corresponding specimen. A question mark (?) indicates plausible haplotypes presented in a specimen from Kamchatka, Himelbrant 2013. Long-spored forms are designated by white allantoid spores; pink ones designate short-spored forms. Specimens collected from conifers are designated by green fir trees. Specimens in blue were collected from Europe and Siberia, specimens in green—from east Asia, specimens in purple—from western North America, and specimens in red—from eastern North America.

Phylogeographic structure.— Since sequences of the protein-coding loci were unavailable for the Australian samples, only the ITS analysis contained them. These Australian samples formed a separate clade represented by *B. mayi* Xue W. Wang & L.W. Zhou and *B. tasmanicum* Xue W. Wang & L.W. Zhou. Apart from the Australian clade, there was a well-supported south Chinese *B. radula* clade nested in the remaining sequences of *B. radula* and *H. syringae* (FIG. 2). In the other gene phylogenies, a south Chinese sample, Härkönen K320, clustered together with *H. syringae*.

The protein-coding loci were geographically structured, as reflected by bifurcations of clades after the deepest split. This indicates populations with a history of genetic isolation. The reverse was observed for a number of geographically distant specimens, which shared nearly identical sequences (FIGS. 3, 4, and 5).

The *gh63* gene tree split all sequences of *B. radula* and *H. syringae* into trans-Beringian and holarctic clades (FIGS. 3 and 4). The trans-Beringian clade was further divided into two well-supported geographic groups: east Asian and North American. The holotype of *H. syringae* from northeast China belonged to the east Asian group of the trans-Beringian clade. The holarctic clade contained samples from eastern North America, Europe, Siberia, and Kamchatka. The extra-American samples formed a Eurasian subclade consisting of genetically similar sequences, with no internal structure, differing at most by a single bp. This suggests gene flow among Eurasian samples.

The *rpb2* gene tree split samples into trans-Beringian and holarctic clades like *gh63* did but placed the samples differently (FIG. 3). Phylogenetically, the trans-Beringian clade was further divided into a temperate-tropical Asian group, to which *H. syringae* belonged, and a west USA-Kamchatka group, samples of which shared identical sequences (FIGS. 3 and 5). In the holarctic clade, six specimens from North America and Eurasia were also genetically very similar (differing by 0–2-bp sites that happened to be phylogenetically informative). One Kamchatka sample, Himelbrant 2013, was polymorphic for all sites distinguishing the two main *rpb2* haplotype groups (TABLE 2) and was not included in the analysis. Considering that we had already detected two haplotypes of *tef1* in Himelbrant 2013, we cautiously assumed that this sample similarly bore both *rbb2* haplotype groups that would have been nested in the two different *rpb2* clades (designated as "?" in FIG. 1).

The *tef1* gene tree uncovered two clades that grouped the preceding samples in different ways (FIGS. 4 and 5). Both clades contained specimens from Asia and North America, but only one of the clades was found in Europe. The clade with only extra-European samples was further divided into North American and east Asian groups. One sample from Kamchatka, Himelbrant 2013, and two from North America, Spirin 8489 and Miettinen 16070, bore both *tef1* haplotypes (designated as α and β in FIGS. 4 and 5), and

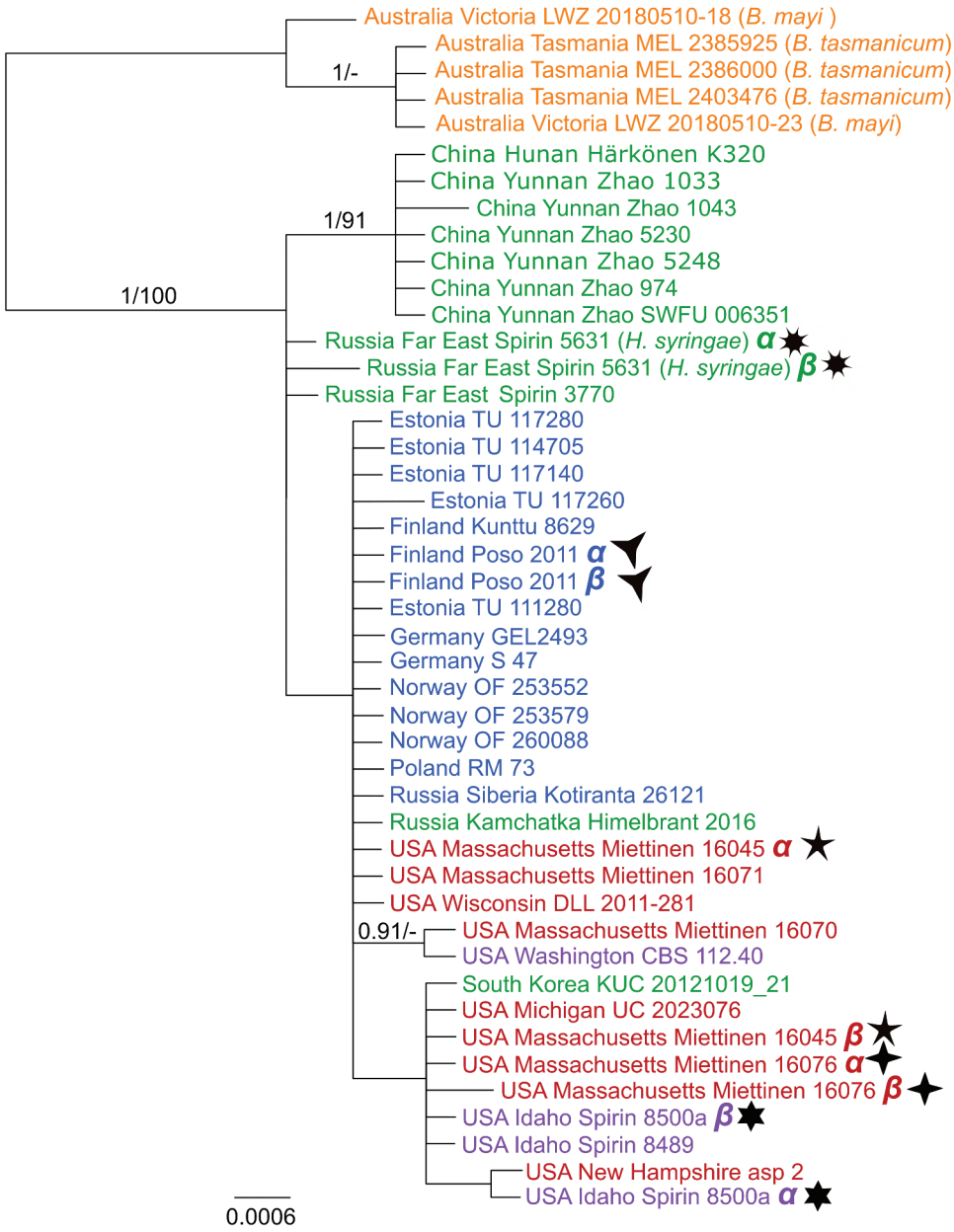

Figure 2. Phylogenetic relationships of *Basidioradulum* inferred from ITS sequences using BI analysis. Bayesian posterior probabilities and ML bootstrap values are shown on nodes; branch lengths reflect estimated number of changes per site. Stars indicate different haplotypes, α and β, present in one specimen. Specimens in blue were collected from Europe and Siberia, specimens in green—east Asia, specimens in purple—western North America, specimens in red—eastern North America, and specimens in yellow—Australia.

they occurred in both clades simultaneously. As with the other loci, the lack of branch length variation suggested that a number of geographically distant sequences were genetically close. Such were also Massachusetts Miettinen 16070 α and Kamchatka Himelbrant 2013 α, the haplotypes retrieved from specimens polymorphic in *tef1*.

Ecology.—There were no clear phylogenetic patterns regarding substrate specificity except that all specimens collected from conifers bore the same *tef1* haplotype group (FIG. 1). However, two out of five conifer-dwelling specimens were polymorphic at *tef1* and also carried another *tef1* haplotype group (FIGS. 1, 4, and 5). Thus, the substrate did not correlate with any phylogenetic structure.

Morphology.—Generally, basidiomata of *H. syringae* and *B. radula* from Asia were robust and often had poroid to semiporoid fertile surfaces as opposed to *B. radula* from Europe and North America. However, there were outliers

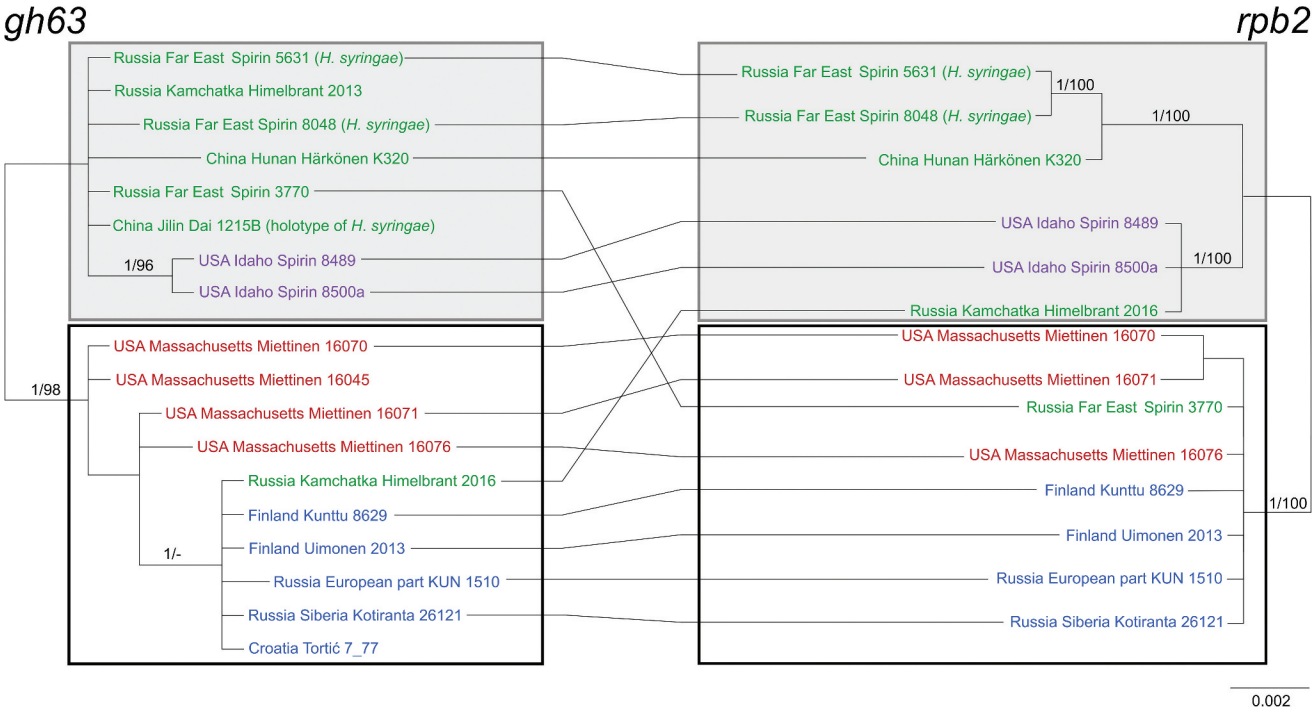

Figure 3. Difference between *gh63* and *rpb2* phylogeny trees inferred from BI analysis. Lines connect the samples of *Basidioradulum radulum* and *Hyphodontia syringae* present in both phylogenies. Bayesian posterior probabilities and ML bootstrap values are shown on nodes; branch lengths reflect estimated number of changes per site. Specimens in blue were collected from Europe and Siberia, specimens in green—from east Asia, specimens in purple—from western North America, and specimens in red—from eastern North America.

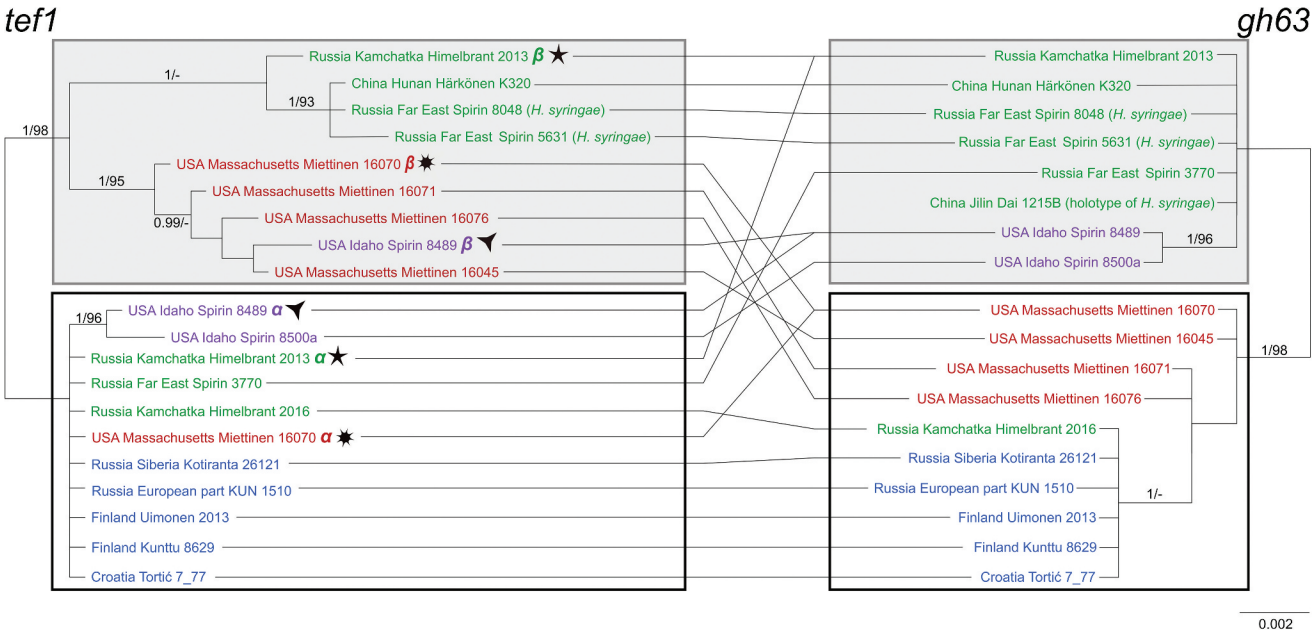

Figure 4. Difference between *gh63* and *tef1* phylogeny trees inferred from BI analysis. Lines connect the samples of *Basidioradulum radulum* and *Hyphodontia syringae* present in both phylogenies. Bayesian posterior probabilities and ML bootstrap values are shown on nodes; branch lengths reflect estimated number of changes per site. Stars indicate different haplotypes, α and β, present in one specimen. Specimens in blue were collected from Europe and Siberia, specimens in green—from east Asia, specimens in purple—from western North America, and specimens in red—from eastern North America.

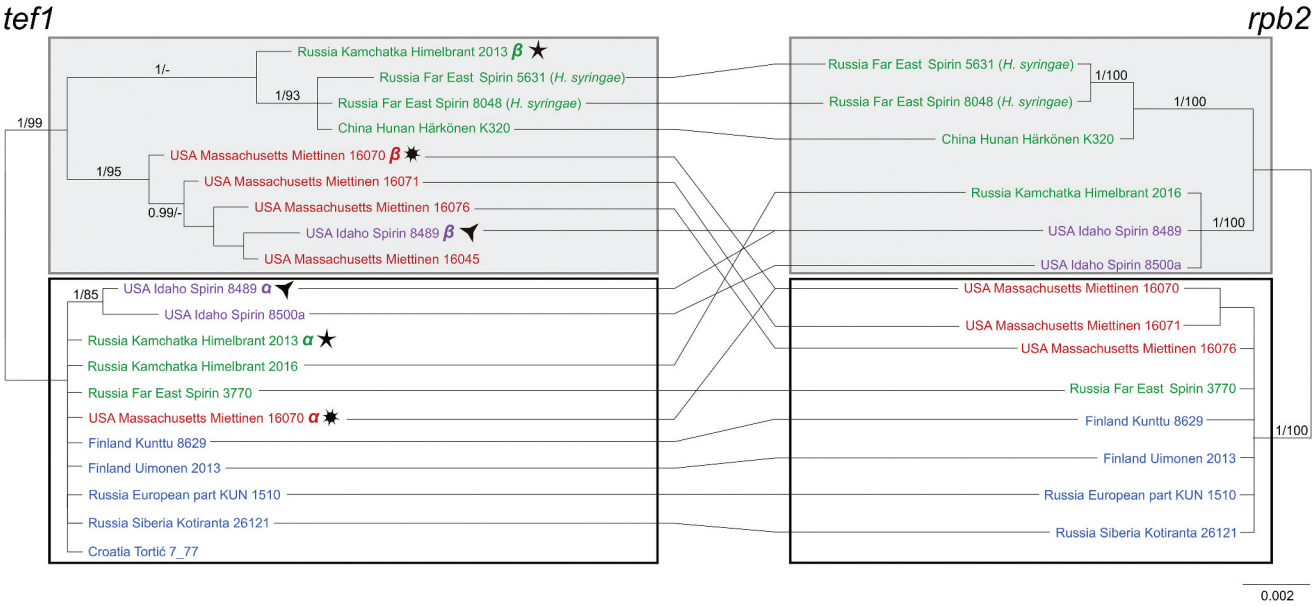

Figure 5. Difference between *tef1* and *rpb2* phylogeny trees inferred from BI analysis. Lines connect the samples of *Basidioradulum radulum* and *Hyphodontia syringae* present in both phylogenies. Bayesian posterior probabilities and ML bootstrap values are shown on nodes; branch lengths reflect estimated number of changes per site. Stars indicate different haplotypes, α and β, present in one specimen. Specimens in blue were collected from Europe and Siberia, specimens in green—from east Asia, specimens in purple—from western North America, and specimens in red—from eastern North America.

and the studied specimens were highly variable (FIG. 6). Microscopic examination showed that different types of hymenial cystidia could be absent or present (TABLE 3), and basidia of different shapes could occur even in the same specimen (FIG. 7; TABLE 3), providing no grounds to divide the specimens into recognizable taxonomic groups. However, we did find one character, basidiospore length, that showed such variance (FIG. 8; TABLE 4). The short-spored form, including most of *H. syringae* examined, dominated in Asia, whereas the long-spored form was characteristic of samples from Europe and North America. These morphological groups best fit the *gh63* phylogeny and its haplotype groups, although outlier individuals undermined this conformity (FIG. 1). The *tef1* gene tree was completely inconsistent with this spore-length-based grouping.

The lack of a clear correspondence between morphology and phylogenetic structure excluded the use of morphological differences as a reliable method to delimit species boundaries in *Basidioradulum*. This was, however, with a proviso that we had not properly studied Australasian collections of *Basidioradulum*. Specifically, we were unable to find any traits suitable for distinguishing *H. syringae* from *B. radula*.

TAXONOMY

The high variability within *Basidioradulum radula* has confused past taxonomists. We are aware of at least nine different names that have been applied to specimens due to perceived differences in basidiomata morphology, basidiospore size, and geographic distribution. Nobles (1967) stabilized the use of names for *Basidioradulum* by proving the conspecificity of synonyms commonly in use at that time. Later, Langer and Dai (1998) described an odontoid to poroid species, *Hyphodontia syringae* Langer, from east Asia, with the holotype collected from *Syringa reticulata* (Oleaceae) or Japanese tree lilac. They assigned this species to the same unranked morphological group (from Langer 1994) as *Hyphodontia quercina* (Pers.) J. Erikss. Later, Malysheva (2006) indicated the morphological similarity of these two species to *B. radula* and assigned both *H. quercina* and *H. syringae* to *Basidioradulum*. In the same year, Larsson et al. (2006) demonstrated the polyphyly of *Hyphodontia* based on DNA evidence: *H. quercina* nested in a well-supported clade that also included several species currently classified as *Xylodon*, whereas *B. radula* formed a clade distant from all *Hyphodontia* in the wide sense (sensu Eriksson 1958). Although Hjortstam and Ryvarden (2009) formally placed *H. syringae* in *Xylodon*, the controversy about the taxonomic placement of this species has lingered to date. The situation was further complicated by Țura et al. (2011), who combined *B. radula* into *Xylodon* in spite of molecular data available at that point showing otherwise.

Our results of four unlinked nuclear loci suggesting gene flow in populations on different continents bluntly excluded dividing *B. radula* by genealogical concordance

Figure 6. Hymenophoral variation in *Basidioradulum radula*. A. Tuberculate (Spirin 8489). B. Raduloid (Viner KUN 1510). C. Abnormal raduloid (Miettinen 23704). D. Poroid (Airaksinen 2006). Bars = 1 cm.

phylogenetic species recognition principles (Taylor et al. 2000). This, together with previous morphological analyses and mating tests on European and North American material of *B. radula* (Nobles 1967), provides ample proof of the intercontinental distribution of the species. Hence, distant populations of *B. radula* constitute a ubiquitous circumboreal species, which allowed us to conclude that *H. syringae* is a younger synonym of *B. radula*.

Specimens examined: AUSTRIA. STEIERMARK: Caranas bei Schwanberg, on *Abies alba*, 22 Feb 1977, *S. Mithelitsch 118* (H7045486). CHINA. HUNAN PROVINCE: Badagongshan National Nature Reserve, on angiosperm branch, 26 Sep 1999, *M. Härkönen K320* (H); JILIN PROVINCE: Changbaishan Nature Reserve, on angiosperm branch, 9 Sep 1995, *Y.C. Dai 1992* (paratype of *Hyphodontia syringae*, H7027689); on *Syringa reticulata*, 7 Sep 1993, *Y.C. Dai 1154* (paratype of *Hyphodontia syringae*, H7027688); 11 Sep 1993, *Y.C. Dai 1215B* (holotype of *Hyphodontia syringae*, H7027700). CROATIA. KRAPINA-ZAGORJE: Donji Macelj, on *Abies alba*, 26 Feb 1977, *M. Tortić 7_77* (H7045538). FINLAND. HELSINKI: Veräjämäki, on *Sorbus aucuparia*, 7 Apr 2020, *O. Miettinen 23704* (H); SOUTH SAVO: Kangasniemi, on *Alnus* sp., 7 Jul 2006, *M.M. Airaksinen 2006* (H6049239); VARSINAIS-SUOMI: Kemiönsaari, Örö, Bataviankorpi, on *Sorbus aucuparia*, 13 May 2015, *P. Kunttu 8629* (H6057703); NOUSIAINEN: Pukkipalo, on *Picea abies*, 19 Oct 2013, *J. Uimonen 2013* (H6042911). RUSSIA. KHABAROVSK REG.: Khabarovsk Dist., Bolshoi Khekhtsir Nature Reserve, on *Acer ukurunduense*, 26 Aug 2014, *V. Spirin 8048* (H7028442); Ulika, on *Syringa amurensis*, 14 Aug 2012, *V. Spirin 5274* (H7023023); Ulun, on *Syringa amurensis*, 26 Aug 2012, *V. Spirin 5631* (H7022783); Solnechnyi Dist., Igdomi, on *Picea ajanensis*, 4 Aug 2011, *V. Spirin 3770* (H7022096); SAKHALIN: Korsakovskiy Rajon, Great Vavayskoye Lake, on *Abies* branch, 23 Aug 2007, *H. Kotiranta 28968* (H7049364); on *Abies* sp., 23 Aug 2007, *H. Kotiranta 28984* (H7049335); KAMCHATKA: Elizovo Dist., Kronotsky Nature Reserve, on *Sorbus sambucifolia*, 11 Aug 2013, *D. E. Himelbrant* 2013 (H); Penzhinsky Dist., Koryak

Table 3. Selected morphological traits of specimens studied.

Specimen	Species	Hymenial surface	Basidia	Capitate cystidia	Moniliform cystidya	Obtuse cystidia
Airaksinen 2006	*B. radula*	Poroid	Clavate	Present	Present	Not found
Dai 1992 (paratype)	*H. syringae*	Poroid	Clavate/suburniform	Present	Present rare (2)	Not found
Dai 1154 (paratype)	*H. syringae*	Raduloid	Clavate	Present	Present	Not found
Dai 1215b (holotype)	*H. syringae*	Raduloid	Clavate/suburniform	Not found	Present	Not found
Härkönen K320	*B. radula*	Raduloid	Clavate	Present rare (6)	Present rare (3)	Present
Himelbrant 2016	*B. radula*	Raduloid	Clavate	Present rare (4)	Not found	Not found
Himelbrant 2013	*B. radula*	Raduloid	Clavate	Not found	Not found	Not found
KUN 1510	*B. radula*	Raduloid	Clavate	Not found	Present	Not found
Kunttu 8629	*B. radula*	Raduloid	Clavate/stalked	Not found	Present	Not found
Miettinen 16076	*B. radula*	Raduloid	Clavate	Present	Present	Present
Mithelitsch 118	*B. radula*	Raduloid	Clavate	Not found	Present	Not found
Nordin 9173	*B. radula*	Raduloid	Clavate	Not found	Present	Present
Spirin 13339	*B. radula*	Raduloid	Clavate/suburniform	Not found	Not found	Not found
Spirin 5274	*H. syringae*	Raduloid	Clavate/suburniform	Present rare (2)	Present rare (2)	Present
Spirin 5631	*H. syringae*	Raduloid	Clavate	Present	Present	Present
Spirin 8048	*B. radula*	Raduloid	Clavate	Present	Present	Not found
Tortić	*B. radula*	Raduloid	Clavate	Present	Present	Not found
Uimonen 2013	*B. radula*	Raduloid	Clavate	Not found	Present rare (3)	Not found
Kotiranta 26121	*B. radula*	Tuberculate	Clavate	Not found	Present	Present
Kotiranta 28968	*B. radula*	Tuberculate	Clavate	Not found	Not found	Present
Kotiranta 28984	*B. radula*	Tuberculate	Clavate	Not found	Not found	Present
Miettinen 16045	*B. radula*	Tuberculate	Clavate/stalked/suburniform	Present	Present	Present
Miettinen 16070	*B. radula*	Tuberculate	Clavate	Present rare (2)	Not found	Present
Miettinen 16071	*B. radula*	Tuberculate	Not found	Not found	Not found	Not found
Miettinen 23704	*B. radula*	Raduloid	Clavate	Not found	Present	Not found
Spirin 3770	*B. radula*	Tuberculate	Clavate	Not found	Not found	Not found
Spirin 8489	*B. radula*	Tuberculate	Not found	Not found	Not found	Not found
Spirin 8500a	*B. radula*	Tuberculate	Not found	Not found	Not found	Not found

Note. If present, each type of microstructures was observed at least 10 times in a specimen; in certain specimens, we could find only a few of capitate and moniliform cystidia, so we give the number of observed structures in parentheses.

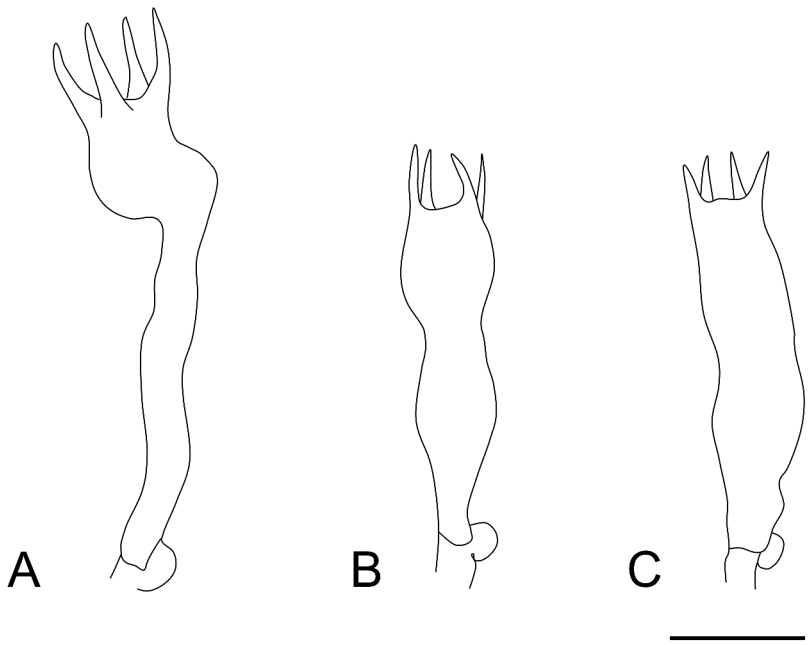

Figure 7. Basidia of *Basidioradulum radula* (Miettinen 16045). A. Stalked. B. Suburniform. C. Clavate. Bar = 10 µm.

Nature Reserve, on *Salix pulchra*, 14 Aug 2016, *D.E. Himelbrant 2016* (H); KRASNOYARSK TERRITORY: Evenk Autonomous District, Central Siberia Nature Reserve, on *Alnus sibirica*, 10 Aug 2013, *H. Kotiranta 26121* (H7024566); TVER OBLAST: Nelidovsky Dist., Central Forest Nature Reserve, on *Populus tremula*, 2 Sep 2015, *I. Viner KUN 1510* (IV). SLOVENIA. GORENJSKA: Kranjska Gora, Vršič, on *Larix decidua*, 27 Sep 2019, *V. Spirin 13339* (H). SWEDEN. GOTHENBURG: Gothenburg Botanical Garden, on *Salix koriyanagi*, 9 Mar 1984, *I. Nordin 9173* (H7045540). USA. IDAHO: Bonner County, Trapper

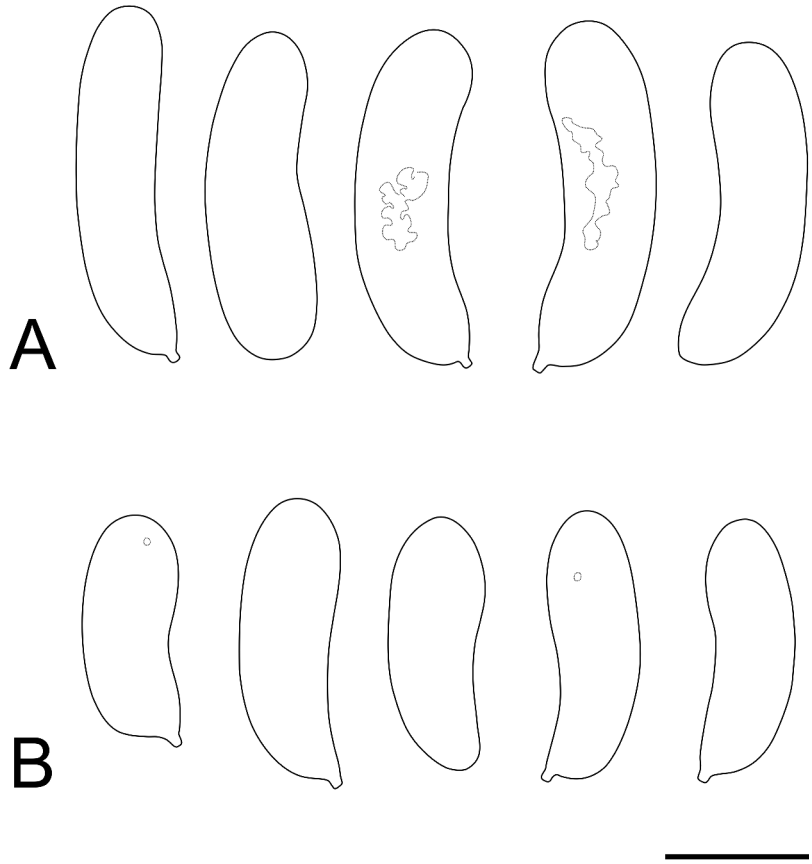

Figure 8. Basidiospores of *Basidioradulum radula*. A. Long-spored form (Kunttu 8629). B. Short-spored form (Spirin 8489). Bar = 5 µm.

Creek, on *Tsuga heterophylla*, 14 Oct 2014, *V. Spirin 8489* (H); *Spirin 8500a* (H); MASSACHUSETTS: Holden, on *Tsuga canadensis*, 21 Apr 2013, *O. Miettinen 16070* (H7005961); Paxton, on angiosperm dead wood, 1 May 2013, *O. Miettinen 16076* (H7005964); Worcester, Columbus Park, on angiosperm branch, 11 Apr 2013, *O. Miettinen 16045* (H7005909); on *Quercus* branch, 22 Apr 2013, *O. Miettinen 16071* (H7005969).

DISCUSSION

Considering the phylogenetic incongruence between all studied DNA loci of *Basidioradulum radula*, a coalescent method may seem appropriate (Degnan and Rosenberg 2009). However, there is an ongoing discussion about the applicability of coalescent models to detect species boundaries especially for populations with allopatric distribution. Several authors (e.g., Sukumaran and Knowles 2017; Leaché et al. 2019) have shown that such models cannot discern a strong population structure from true speciation. In our opinion, this hampers utilizing coalescent models in our case where we deal with a collection of recently diverged populations. Therefore, we analyzed the DNA loci separately, following genealogical concordance phylogenetic species recognition principles and considering substrate specificity, morphological, and geographic data. We believe that our results combined with previously published mating experiments (Nobles 1967) suffice well for a reliable conclusion on the taxonomic status of *B. radula* and *Hyphodontia syringae*.

We demonstrated here that the DNA loci of *B. radula* are geographically structured, which means that the history of genetic isolation in its diverged populations is long enough to accumulate detectable genetic differences. We also showed that sequences from the same geographic area often pertain to different haplotype groups. Such a pattern alone might be a result of incomplete lineage sorting in recently emerged species. However, we also found clear signs of gene flow between populations, which favor a single-species interpretation.

For example, Massachusetts Miettinen 16070, polymorphic at *tef1*, bears haplotype α, which is nearly identical to a number of specimens from Eurasia. At the same time, its counterpart Miettinen 16070 β clusters together with other American sequences. The incomplete lineage sorting interpretation implies that North American Miettinen 16070 α and the Eurasian *tef1* haplotypes were independently inherited from an ancestral population before the split. Scattered in populations on different continents, these

Table 4. Specimens examined for this study and their spore measurements.

Specimen	Species	Area	L′	L	W′	W	Q′	Q	n
Long-spored form									
Airaksinen 2006	*B. radula*	Finland	(5.1–)7.1–10.9(–11.3)	9.3	(2.8–)2.9–3.6(–3.7)	3.2	(1.8–)2.1–3.5(–3.7)	2.9	30
Dai 1992(–paratype)	*H. syringae*	Northeast China	(6–)7.7–9.4(–9.7)	8.6	2.8–3.2(–3.3)	3	(2.1–)2.6–3.2	2.9	30
Himelbrant 2016	*B. radula*	Russian Kamchatka	8.1–10.7(–11.3)	9.7	2.7–3.2	3	(2.7–)2.8–3.6	3.3	30
KUN 1510	*B. radula*	Russian Eastern Europe	(6.9–)7.2–10.6(–11.1)	8.6	(2.5–)2.7–3.3(–3.5)	2.9	2.5–3.9(–4)	3	30
Kunttu 8629	*B. radula*	Finland	(7–)7.3–11.3(–13.1)	9.5	(2.3–)2.4–3.8(–3.9)	3.2	(2.3–)2.5–3.5(–3.8)	3	30
Miettinen 16045	*B. radula*	Eastern USA	(7–)7.1–10.2(–10.3)	8.9	(2.8–)2.9–4(–4.1)	3.4	(2–)2.2–3.1(–3.2)	2.6	30
Miettinen 16070	*B. radula*	Eastern USA	(5.5–)6–10.6(–11)	8.8	(2–)2.2–4(–4.8)	3.3	(1.9–)2–4.1(–4.5)	2.8	30
Miettinen 16071	*B. radula*	Eastern USA	8–10(–10.1)	9.1	(3.2–)3.4–4.1	3.8	2–2.7(–2.8)	2.4	30
Miettinen 16076	*B. radula*	Eastern USA	(6.6–)7.2–9.6(–10.7)	8.6	(2.6–)2.8–3.7(–3.9)	3.2	(2–)2.3–3(–3.4)	2.7	30
Miettinen 23704	*B. radula*	Finland	(8.2–)8.9–12.4(–12.8)	10.5	(2.4–)2.8–3.8(–3.9)	3.2	(2.6–)2.8–3.7(–4)	3.3	30
Mithelitsch 118	*B. radula*	Austria	(9.2–)9.3–11.1(–13)	10.2	(2.5–)2.7–3.8(–4)	3.2	(2.6–)2.7–3.8(–4.1)	3.2	30
Nordin 9173	*B. radula*	Sweden	(6.7–)8.2–11.6(–12.4)	10	(2.2–)2.7–3.7(–4)	3.1	(2.2–)2.5–3.9(–4.1)	3.2	30
Spirin 13339	*B. radula*	Slovenia	(7.9–)8.4–10.6(–11)	9.4	2.7–3.1(–3.2)	2.9	(2.7–)2.8–3.7(–3.9)	3.2	30
Spirin 5631	*H. syringae*	Russian Far East	(6.7–)7.4–12.8(–13.2)	9.6	(2.2–)2.6–3.6(–3.7)	3	(2.5–)2.6–3.8(–3.9)	3.2	30
Spirin 8500a	*B. radula*	Western USA	(8.5–)8.9–11(–12.4)	10	2.8–4.1(–8.6)	3.6	(1.1–)2.4–3.4	2.9	30
Tortić 7_77	*B. radula*	Croatia	(7–)9.1–11.5(–13)	10	(2.6–)2.7–3.2(–5.7)	3	(2.3–)2.7–3.8(–4)	3.4	32
Uimonen 2013	*B. radula*	Finland	(8.1–)8.7–10(–10.2)	9.3	(2.1–)2.2–3(–3.1)	2.7	(2.9–)3–4.3(–4.7)	3.5	30
Short-spored form									
Dai 1154(–paratype)	*H. syringae*	Northeast China	(6.9–)7–9.4(–10.5)	8	(2.5–)2.6–3(–3.2)	2.9	(2.3–)2.4–3.2(–3.3)	2.8	30
Dai 1215B Holotype	*H. syringae*	North-East China	(7.2–)7.6–9(–9.1)	8.4	2.9–3.2	3	(2.4–)2.5–3(–3.1)	2.8	30
Härkönen K320	*B. radula*	Southern China	(7.2–)7.5–9.1(–9.2)	8.4	(2.5–)2.7–3(–3.1)	2.9	(2.5–)2.6–3.2(–3.5)	2.9	30
Himelbrant 2013	*B. radula*	Russian Kamchatka	(5–)5.2–8.9(–9.1)	7.6	(2.8–)2.9–3.7(–4.1)	3.3	(1.3–)1.6–2.8(–2.9)	2.3	34
Kotiranta 26121	*B. radula*	Russian Siberia	(6.8–)6.9–9(–9.4)	7.9	(2.5–)2.6–3.1(–5.9)	3	(1.2–)2.4–3.2(–3.3)	2.7	30
Kotiranta 28968	*B. radula*	Russian Far East	(6.8–)7–8.8(–9)	7.8	2.5–3.3(–3.5)	2.9	(2.2–)2.3–3(–3.1)	2.7	30
Kotiranta 28984	*B. radula*	Russian Far East	(6.7–)6.9–9.1	7.9	(2.5–)2.6–3.3(–4)	3	(1.7–)2.2–3.1(–3.4)	2.6	30
Spirin 3770	*B. radula*	Russian Far East	(5.4–)5.9–8.5(–8.8)	7	(2.4–)2.6–3.9	3.1	(1.6–)1.8–2.7(–2.9)	2.3	30
Spirin 5274	*H. syringae*	Russian Far East	(6.8–)6.9–9.1(–9.7)	7.8	2.6–3.1(–3.2)	2.9	2.3–3.2	2.7	32
Spirin 8048	*B. radula*	Russian Far East	6.8–8.7(–9.3)	7.7	(2.8–)2.9–3.6(–3.7)	3.3	(2–)2.1–2.8(–3)	2.4	30
Spirin 8489	*B. radula*	Western USA	(5.9–)6.2–9(–9.1)	7.6	2.8–3.7(–4)	3.2	2–2.9(–3)	2.4	30
Average			(5–)6.8–10.9(–13.2)	8.8	(2–)2.6–3.8(–8.6)	3.1	(1.1–)2.2–3.7(–4.7)	2.9	848

haplotypes should have accumulated enough differences so that the resulting clade would have shown some internal structure such as branch length variation and further splitting of geography-specific clades. This is not the case; thus, we interpret two different haplotype groups in Miettinen 16070 as a result of a hybridization event. We describe several similar cases of apparent gene flow in the results. Moreover, the complex genetic pattern observed in *B. radula* is likely a result of introgression, as there were no specimens polymorphic across all studied loci, i.e., probable first generation hybrids.

We find the following interpretation to be credible. The ancestral population of *B. radula* underwent geographic speciation, but gene flow between the progeny populations was restored later, hindering complete speciation. This model fits well the cycle of climate and environmental changes during the Quaternary: vicariance may have been caused by the flooding of Beringia and advancing ice shields, whereas reverse introgression may have been promoted by the reestablishment of forest belts and even international wood trade. To validate this interpretation, a proper characterization of *B. radula* population structure would be required. This could be done with the aid of coalescent-based models, network analyses, and denser sampling around the globe, but such an approach fell out of the scope of our taxonomically oriented study.

Many species-level taxonomic papers of Agaricomycetes still rely on one or two unlinked phylogenetic loci, usually nuc rRNA and one protein-coding gene. When species are not very closely related and morphological differences are plentiful and consistent, then this approach is still acceptable. In the case of species complexes of closely related species, we need to update our standards of species recognition. We demonstrate here that sometimes the reliance on such a limited number of loci in taxonomic treatments of fungi with minor morphological differences can create alternative scenarios of how to delimit species. If we had not taken into account multiple gene tree histories and/or samples of *Basidioradulum radula*, there would have been a number of ways to shuffle analyzed samples so that at least two species could be distinguished. For instance, if the *gh63* gene tree were interpreted alone, this would have shown two species recognizable by basidiospore size. If we had ignored samples with corresponding polymorphic loci, the *tef1* phylogeny would have suggested another species concept based on geographic structure and substrate preference. One species would have been an angiosperm-dwelling specialist distributed in east Asia and North America. The other species would have been a generalist with a circumboreal distribution, but only European and Siberian populations would have occurred on angiosperm wood.

Thus, when dealing with species delimitation of morphologically and phylogenetically closely related Agaricomycete species, addressing incongruence of gene phylogenies is needed. However, the actual number of loci needed to resolve species in such cases depends upon lineage age, demographic history, and population size and thus differs case by case. Based on our results, we suggest an initial test of incongruence among phylogenies of three unlinked DNA loci on a comprehensive set of specimens. By a comprehensive set, we mean an intercontinental sampling that encompasses north-south and east-west directions so that vicariance created by climate and geographic barriers can be taken into account. In cases of suspected incongruence between the gene phylogenies, a fourth locus (or more) should be analyzed in order to adopt a taxonomic conclusion.

Of course, this is an ideal approach. In practice, such sampling might be hampered by multiple factors—sampling intensity, quality, and age of specimens. Moreover, laboratories vary in expertise and funds available to produce such data. But having such a standard shows room for improvement. We conclude that a plethora of systematic studies of wood-decaying Agaricomycetes would have benefited from the use of this strategy.

Recently, Wang et al. (2020) described *Basidioradulum mayi* and *B. tasmanicum* as two separate species despite the fact that their ITS phylogeny did not resolve them as two separate clades, reaffirmed by our ITS analysis (FIG. 2). Besides that, only the spore variation range of *B. tasmanicum* slightly exceeds the known limits of *B. radula*, whereas all other traits distinguishing their new species fall within the variability of *B. radula* (TABLES 3 and 4). In light of our results, based on several unlinked DNA markers, as well as morphological analyses, morphological species recognition in this group is problematic. Thus, recognition of *B. mayi* and *B. tasmanicum* as separate species is questionable.

ACKNOWLEDGMENTS

We thank the editor, Dr. Patrick B. Matheny, and the anonymous reviewers of the manuscript for their useful comments. Evgeniy Dunayev (Young Naturalist Club of the Zoological Museum, Moscow University, Russia), Irina Stepanchikova, and Dmitry Himelbrant (Saint Petersburg) kindly provided us with valuable fungal collections.

FUNDING

This research was supported by a University of Helsinki three-year research project (O.M., I.V.), Societas pro Fauna et Flora Fennica (I.V.), and Moscow State University Grant for Leading Scientific Schools "Depository of the Living Systems" in framework of the MSU Development Program (L.K.).

ORCID

Ilya Viner http://orcid.org/0000-0002-5193-7720
Lyudmila Kokaeva http://orcid.org/0000-0003-1384-3552
Viacheslav Spirin http://orcid.org/0000-0001-5436-6997
Otto Miettinen http://orcid.org/0000-0001-7502-710X

LITERATURE CITED

Chang CT, Tsai CN, Tang CY, Chen CH, Lian JH, Hu CY, Tsai CL, Chao A, Lai CH, Wang TH, Lee YS. 2012. Mixed sequence reader: a program for analyzing DNA sequences with heterozygous base calling. The Scientific World Journal 2012:1–10.

Degnan JN, Rosenberg NA. 2009 Gene tree discordance, phylogenetic inference and the multispecies coalescent. Trends in Ecology & Evolution 24:332–340.

Dmitriev DA, Rakitov RA. 2008. Decoding of superimposed traces produced by direct sequencing of heterozygous indels. PLoS Computational Biology 4:e1000113.

Eriksson J. 1958. Studies in the Heterobasidiomycetes and Homobasidiomycetes—Aphyllophorales of Muddus National Park in North Sweden. Symbolae Botanicae Upsalienses 16:1–172.

Gardes M, Bruns TD. 1993. ITS primers with enhanced specificity for basidiomycetes—application to the identification of mycorrhizae and rusts. Molecular Ecology 2:113–118.

Giraud T, Refrégier G, Le Gac M, de Vienne DM, Hood ME. 2008. Speciation in fungi. Fungal Genetics and Biology 45:791–802.

Hjortstam K, Ryvarden L. 2009. A checklist of names in *Hyphodontia* sensu stricto-sensu lato and *Schizopora* with new combinations in *Lagarobasidium, Lyomyces, Kneiffiella, Schizopora*, and *Xylodon*. Synopsis Fungorum 26:33–55.

Holder MT, Anderson JA, Holloway AK. 2001. Difficulties in detecting hybridization. Systematic Biology 50:978–982.

Katoh K, Rozewicki J, Yamada KD. 2017. MAFFT online service: multiple sequence alignment, interactive sequence choice and visualization. Briefings in Bioinformatics 20:1160–1166.

Kearse M, Moir R, Wilson A, Stones-Havas S, Cheung M, Sturrock S, Buxton S, Cooper A, Markowitz S, Duran C, Thierer T, Ashton B, Meintjes P, Drummond A. 2012. Geneious Basic: an integrated and extendable desktop software platform for the organization and analysis of sequence data. Bioinformatics 28:1647–1649.

Langer E. 1994. Die Gattung *Hyphodontia* John Eriksson. Bibliotheca Mycologica 154:1–298.

Langer E, Dai YC. 1998. Changbai wood-rotting fungi 8. *Hyphodontia syringae* sp. nov. Mycotaxon 67:181–190.

Larsson KH, Parmasto E, Fischer M, Langer E, Nakasone KK, Redhead SA. 2006. Hymenochaetales: a molecular phylogeny for the hymenochaetoid clade. Mycologia 98:926–936.

Leaché AD, Zhu T, Rannala B, Yang Z. 2019. The spectre of too many species. Systematic Biology 68:168–181.

Leigh JW, Susko E, Baumgartner M, Roger AJ. 2008. Testing congruence in phylogenomic analysis. Systematic Biology 57:104–115.

Malysheva VF. 2006. Notes on rare species of aphyllophoroid fungi found in Zhiguli Nature Reserve (Samara Region, European Russia). Karstenia 46:25–32.

Matheny PB. 2005. Improving phylogenetic inference of mushrooms with RPB1 and RPB2 nucleotide sequences (*Inocybe*; Agaricales). Molecular Phylogenetics and Evolution 35:1–20.

Miettinen O, Niemela T, Spirin W. 2006. Northern *Antrodiella* species: the identity of *A. semisupina*, and type studies of related taxa. Mycotaxon 96:211–240.

Milne I, Lindner D, Bayer M, Husmeier D, McGuire G, Marshall DF, Wright F. 2008. TOPALi v2: a rich graphical interface for evolutionary analyses of multiple alignments on HPC clusters and multi-core desktops. Bioinformatics 25:126–127.

Nobles MK. 1967. Conspecificity of *Basidioradulum* (*Radulum*) *radula* and *Corticium hydnans*. Mycologia 59:192–211.

Pérez-Izquierdo L, Morin E, Maurice JP, Martin F, Rincón A, Buée M. 2017. A new promising phylogenetic marker to study the diversity of fungal communities: the Glycoside Hydrolase 63 gene. Molecular Ecology Resources 17:1–11.

Rehner SA, Buckley E. 2005. A *Beauveria* phylogeny inferred from nuclear ITS and EF1-α sequences: evidence for cryptic diversification and links to *Cordyceps* teleomorphs. Mycologia 97:84–98.

Rehner SA, Samuels GJ. 1994. Taxonomy and phylogeny of *Gliocladium* analysed from nuclear large subunit ribosomal DNA sequences. Mycological Research 98:625–634.

Ronquist F, Teslenko M, Van Der Mark P, Ayres DL, Darling A, Höhna S, Larget B, Liu L, Suchard M, Huelsenbeck JP. 2012. MrBayes 3.2: efficient Bayesian phylogenetic inference and model choice across a large model space. Systematic Biology 61:539–542.

Stamatakis A. 2006. RAxML-VI-HPC: maximum likelihood-based phylogenetic analyses with thousands of taxa and mixed models. Bioinformatics 22:2688–2690.

Sukumaran J, Knowles LL. 2017. Multispecies coalescent delimits structure, not species. Proceedings of the National Academy of Sciences of the United States of America 114:1607–1612.

Taylor JW, Jacobson DJ, Kroken S, Kasuga T, Geiser DM, Hibbett DS, Fisher MC. 2000. Phylogenetic species recognition and species concepts in fungi. Fungal Genetics and Biology 31:21–32.

Ţura D, Zmitrovich IV, Wasser SP, Spirin WA, Nevo E. 2011. Biodiversity of Heterobasidiomycetes and non-gilled Hymenomycetes (former Aphyllophorales) of Israel. Ruggell, Liechtenstein: ARA Gantner. 566 p.

Vilgalys R, Hester M. 1990. Rapid genetic identification and mapping of enzymatically amplified ribosomal DNA from several *Cryptococcus* species. Journal of Bacteriology 172:4238–4246.

Wang XW, Jiang JH, Zhou LW. 2020. *Basidioradulum mayi* and *B. tasmanicum* spp. nov. (Hymenochaetales, Basidiomycota) from both sides of Bass Strait, Australia. Scientific Reports 10:102.

White TJ, Bruns T, Lee S, Taylor JW. 1990. Amplification and direct sequencing of fungal ribosomal RNA genes for phylogenetics. In: Innis MA, Gelfand DH, Sninsky JJ, White TJ, eds. PCR protocols: a guide to the methods and applications. New York: Academic Press. p. 315–322.

Zhidkov I, Cohen R, Geifman N, Mishmar D, Rubin E. 2011. CHILD: a new tool for detecting low-abundance insertions and deletions in standard sequence traces. Nucleic Acids Research 39:1–8.